Recovery of Periodic Signals in Event Camera Data: Theory and Empirical Results

Mark J. Moretto
North Carolina State University
Katherine Melbourne, Marcus J. Holzinger
University of Colorado Boulder

ABSTRACT

Event cameras report discrete events signifying a change in voltage of the detectors circuits. Event cameras can be used to recover the vibrational modes and rotational state of satellites and debris. In space situational awareness this information can be used to disambiguate observations and to infer the operational mode of a satellite. This work quantifies the sensitivity to and recoverability of periodic signals from event camera data to inform the design and tuning of these devices, as well as demonstrates these results on empirical data.

1. INTRODUCTION

Space situational awareness (SSA) requires the correlation of measurements to specific objects debris or spacecraft. The rotational state and vibrational modes of these objects can help resolve ambiguities in this association process and provide additional information about the properties and operational state of the object. Event, also known as neuromorphic, cameras have shown promise in rapidly quantifying the rotation and vibration of spacecraft from ground-based observations [2, 1].

Event cameras are collections of circuits that are sensitive to changes in flux and that operate independently [4]. The circuits report events when the voltage changes by plus or minus a tunable percentage threshold, generating positive or negative events, respectively. Events are reported with microsecond precision. Benson & Holzinger [2, 1] derived equations for the mean voltage under certain periodic signals, as well as providing proof-of-concept analysis of observations of the ISS [2] and Ajisai [2, 1]. The goal of this work is to quantify the sensitivity to and recoverability of periodic signals from event camera data to inform the design and tuning of these devices, as well as to demonstrate these results on empirical data.

This paper presents a frequency domain controls analysis of the event camera circuit and uses those results combined with insights from the equations derived by Benson & Holzinger [2, 1] to quantify the recoverability of periodic signals from event camera data. Next, idealized event data are simulated, analytical event rates are calculated, and a proxy voltage is reconstructed from event data. These quantities are used to analyze the frequency spectrum of the event data using Fast Fourier Transforms (FFTs) and provide insights into the relationship between those spectra and the frequency content of the input signal. Finally, event data from the VADeR Lab observatory, which has been acquiring event data of Low Earth Orbit (LEO) and Geostationary Earth Orbit (GEO) satellites, is analyzed using multiple methods to attempt to pull signal out of data from an average satellite.

2. EVENT CAMERA MODEL

From Benson & Holzinger [2, 1] the mean voltage in an event camera circuit can be written as:

$$\frac{d\bar{V}(t)}{dt} = -a\bar{V}(t) + b\ln\left(\lambda(t)/\lambda_r\right) \ , \tag{1}$$

where t is time, $\bar{V}$ is the mean voltage, λ is the incident flux, λ_r is the reference flux, a is the decay rate, and b is the gain of the circuit. Events are tripped when:

$$e_+ \text{ if } V(t) \geq V(t_i)(1+\delta) \,, \tag{2}$$

$$e_- \text{ if } V(t) \leq V(t_i)(1-\delta) \,, \tag{3}$$

where t_i is the time of the previous event and δ is the fractional change required to trip an event. e_+ and e_- are positive and negative events, often represented by $+1$ and -1, respectively.

3. TRANSFER FUNCTION

This work is concerned with the recovery of periodic signals, which suggests that a classical controls approach can be worthwhile. A transfer function for the mean voltage can be derived. First, Equation 1 is rearranged:

$$\frac{d\bar{V}(t)}{dt} = -a\bar{V}(t) + b\ln(\lambda(t)) - b\ln(\lambda_r) \,, \tag{4}$$

and the input signal can be defined as:

$$m(t) = \ln(\lambda(t)) \,. \tag{5}$$

Taking the Laplace transform of Equation 4 subject to the input signal $m(t)$ yields:

$$s\bar{V}(s) - \bar{V}(t=0) = -a\bar{V}(s) + bm(s) - b\frac{\ln(\lambda_r)}{s} \,. \tag{6}$$

Setting the initial conditions equal to zero and rearranging:

$$\bar{V}(s)(s+a) = bm(s) - b\frac{\ln(\lambda_r)}{s} \,. \tag{7}$$

In order to remove the constant term on the left hand side and force a zero-mean sinusoidal input it is convenient to set

$$m(t) = m_{sin}(t) + \ln(\lambda_r) \,, \tag{8}$$

where $m_{sin}(t)$ is of the form:

$$m_{sin}(t) = A\sin(\omega t - \theta) \,, \tag{9}$$

where A, ω, and θ are constants. It is not necessary to specify the specific form of the sinusoidal input to analyze the frequency response of the system. The Laplace transform of $m(t)$ can be written as:

$$m(s) = m_{sin}(s) + \frac{\ln(\lambda_r)}{s} \,. \tag{10}$$

Using this input in Equation 7 results in:

$$\bar{V}(s)(s+a) = bm_{sin}(s) \,. \tag{11}$$

Now the transfer function can be recovered:

$$\frac{\bar{V}(s)}{m_{sin}(s)} = \frac{b}{s+a} = \frac{b/a}{s/a+1} \tag{12}$$

The transfer function provides analytical insights into the behavior of the event camera circuit. The most important insight is that the transfer function has one pole and the location of that pole determines the limiting frequency that the voltage is most sensitive too. In this case:

$$\omega_{max} = a \, . \tag{13}$$

It it also noteworthy that the magnitude of the voltage change depends on b/a; therefore, increasing a will also decrease the amplitude of the signal. Benson & Holzinger [2, 1] note that increasing a decreased the sensitivity to periodic signals in their simulations and these results are consistent with the decreased amplitude of the voltage change. The event camera does not report the voltage, rather events are triggered by the change in voltage. If the magnitude of the change in voltage is not sufficient to trigger an event then the periodic signal in the voltage will remain undetected even if present in the circuit.

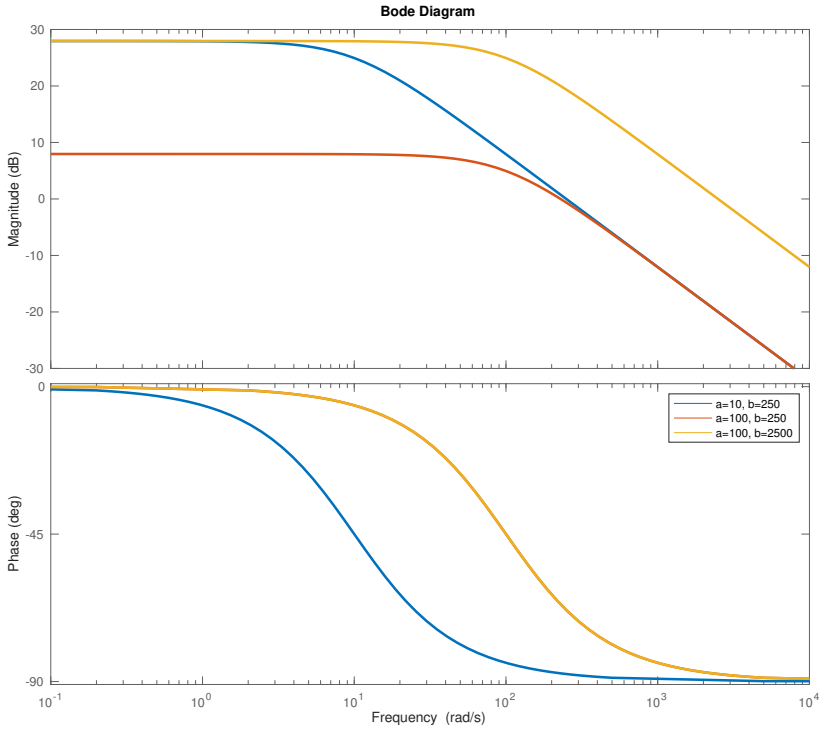

Fig. 1: Bode diagram for the event camera circuit transfer function.

Fig. 1 depicts the Bode diagram for the event camera circuit transfer function for three combinations of gains and decay rates. Note that increasing the decay rate by an order of magnitude decreases the magnitude of the output voltage by 20 decibels. Compensating for this by increasing the gain by an order of magnitude results in the original output magnitude, as expected. The phase offset between the input and output frequencies only depends on the decay rate, a.

4. AMPLITUDE TO REFERENCE VOLTAGE ANALYSIS

Benson & Holzinger [2, 1] derived analytical equations for the mean voltage in an event camera circuit subject to a Fourier series input in stellar magnitudes. The equation of motion for the mean voltage becomes:

$$\frac{d\bar{V}(t)}{dt} = -a\bar{V}(t) - \frac{2}{5}\ln(10)b\ln\left(\lambda(t)\right) - b\ln\left(\lambda_r\right) \ , \tag{14}$$

and the input $m(t)$ can be written as:

$$m(t) = c_0 + \sum_{n=0}^{N}\left[a_n\cos(n\omega t) + b_n\sin(n\omega t)\right] \ . \tag{15}$$

Benson & Holzinger [] solved for the mean voltage in steady state as:

$$\bar{V}_{ss}(t) = -\frac{b}{a}\left(\frac{2}{5}\ln(10)c_0 + \ln(\lambda_r\right) \tag{16}$$
$$-\frac{2}{5}\ln(10)b\sum_{n=1}^{n}\frac{(aa_n - n\omega b_n)\cos(n\omega t) + (n\omega a_n + ab_n)\sin(n\omega t)}{a^2 + n^2\omega^2} \ .$$

The steady state mean voltage can be separated into constant, $\bar{V}_{ss,0}(t)$, and periodic components, $\bar{V}_{ss,p}(t)$:

$$\bar{V}_{ss,0}(t) = -\frac{b}{a}\left(\frac{2}{5}\ln(10)c_0 + \ln(\lambda_r)\right) \ , \tag{17}$$

$$\bar{V}_{ss,p}(t) = -\frac{2}{5}\ln(10)b\sum_{n=1}^{n}\frac{(aa_n - n\omega b_n)\cos(n\omega t) + (n\omega a_n + ab_n)\sin(n\omega t)}{a^2 + n^2\omega^2} \ . \tag{18}$$

It is insightful to investigate the input:

$$m(t) = c_0 + a_1\cos(\omega t) \ , \tag{19}$$

where the resulting steady state periodic term simplifies to:

$$\bar{V}_{ss,p}(t) = -\frac{2}{5}\ln(10)b\frac{aa_1\cos(\omega t) + \omega a_1\sin(\omega t)}{a^2 + \omega^2} \ . \tag{20}$$

The magnitude of the oscillations can be written as:

$$A_V = \frac{2}{5}\ln(10)b\frac{\sqrt{a^2a_1^2 + \omega^2a_1^2}}{a^2 + \omega^2} \ , \tag{21}$$

which simplifies to:

$$A_V = \frac{2}{5}\ln(10)b\frac{|a_1|}{\sqrt{a^2 + \omega^2}} \ . \tag{22}$$

Now the ratio of the variations in voltage to the constant term can be calculated:

$$\frac{A_V}{|\bar{V}_{ss,0}|} = \frac{\frac{2}{5}\ln(10)b\frac{|a_1|}{\sqrt{a^2+\omega^2}}}{\left|\frac{b}{a}\left(\frac{2}{5}\ln(10)c_0 + \ln(\lambda_r)\right)\right|} = \frac{a\frac{|a_1|}{\sqrt{a^2+\omega^2}}}{\left|\left(c_0 + \frac{\ln(\lambda_r)}{\frac{2}{5}\ln(10)}\right)\right|} \ . \tag{23}$$

This indicates that the gain of the circuit does not directly impact the mean fractional change of the voltage from a periodic signal in stellar magnitudes. The reference flux can be set such that $\ln(\lambda_r) = 0$ resulting in:

$$\frac{A_V}{|\bar{V}_{ss,0}|} = \frac{a|a_1|}{|c_0|\sqrt{a^2+\omega^2}} \,. \tag{24}$$

For a given frequency ω, Equation 24 asymptotically approaches a value of $|a_1/c_0|$ as a goes to infinity. Similarly it will equal 0 for $a = 0$. This implies that larger values for the decay rate will result in larger relative changes in the voltage; however, the proportion of the voltage change is limited by the ratio of the object's brightness variations relative to the mean brightness and the reference flux. Equation 24 also implies that the change in voltage needed to trigger an event should be small and the maximum threshold can be determined from this analysis. Note that this neglects the stochastic nature of the incoming photons and this the voltage in the event camera circuit. The signal to noise ratio and the conversion from voltage to events should be studied in future work.

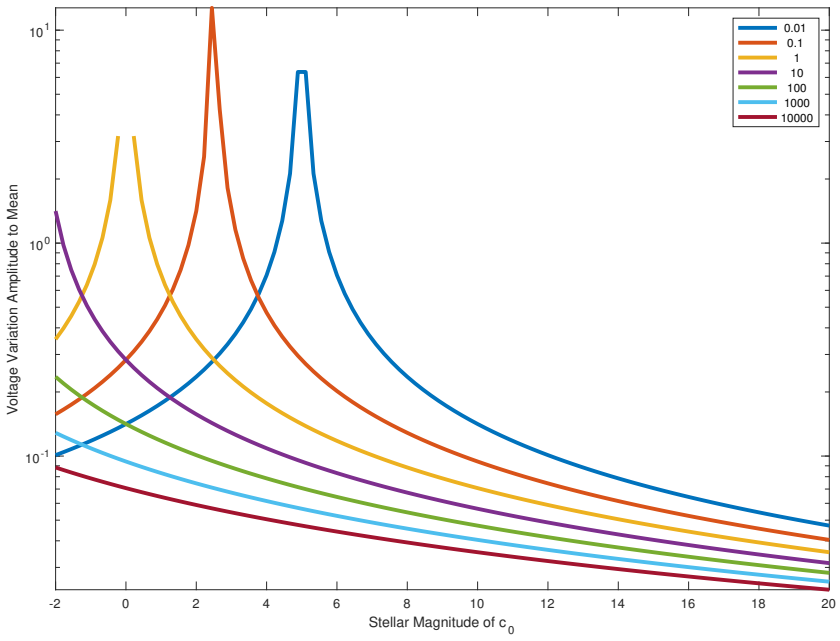

Fig. 2: Voltage variation amplitude to mean voltage ratio for $a = 10$, $\omega = 10$, and $b = 250$ for differing values of the reference flux as denoted in the legend and a one stellar magnitude amplitude variation.

Fig. 2 shows the relationship between the ratio of the voltage oscillation magnitude to it's mean and the mean stellar magnitude of the object for different values of the reference flux and a one stellar magnitude amplitude variation. Note that the large spikes in the ratio are where the mean voltage goes to zero. For comparison, Benson et al. [3] observed changes of one to several stellar magnitudes in GEO satellite lightcurves.

5. RECOVERY OF EVENTS FROM SIMULATED DATA

One of the largest hurdles to detecting periodic signals in event camera data is understanding how the frequency content of the voltage signal is transformed as it is converted to events. In this section, idealized events will be calculated numerically from the steady state mean voltage. Next, an analytical event rate will be presented. Finally a proxy voltage will be used to approximate the voltage from event data. To investigate the recovery of frequency content from event data the frequency content of these three signals will be compared to the known truth.

5.1 Events

The simulation of events for this work differs from that of Benson & Holzinger [2, 1] in that they simulated stochastic events whereas these idealized events are deterministic from the mean steady state voltage. An initial event voltage

is chosen and then the mean voltage, looking forward in time, is compared to the reference voltage until an event is tripped according to Equations 2 and 3, which reset the event voltage to the voltage at which the event was tripped. These events are deterministic from the voltage history and initial event voltage. Some error will be accumulated as the events are not tripped mid-timestep where the voltage and triggering voltage would first coincide. The timestep used in this section was 1×10^{-4} seconds. Event cameras have approximately sub-milisecond timing precision [4] and the Prophesee EV3 GEN4.1 reports times to the microsecond.

5.2 Analytical Event Rates (dV/V)

The times of idealized events has not be readily predicted analytically and the discretization of the voltage into events can be expected to distort the frequency content of the voltage. It is helpful to define a mean event rate, $n_e(t)$, which is the number of events per unit time at a given time. One can recognize that the mean event rate is proportional to the time derivative of the mean voltage divided by the instantaneous mean voltage:

$$n_e(t) \sim \frac{\frac{d\bar{V}_{ss}}{dt}}{\bar{V}_{ss}} \tag{25}$$

Remember that both $\frac{d\bar{V}_{ss}}{dt}$ and $\bar{V}_{ss}$ have analytical solutions when the input flux, in stellar magnitudes, is expressed as a Fourier series. Both the derivative, Equation 14, and the mean voltage, Equation 16, have periodic term it is expected that some beating will occur.

5.3 Reconstructed Voltage History

As noted by Benson & Holzinger [2], the voltage normalized by the initial event voltage can be approximated from the event history as:

$$\frac{V_n}{V_0} = \prod_{i=1}^{n} (1 + e_i \delta) \ , \tag{26}$$

where e_i is the polarity of the i^{th} event and δ is the fractional change necessary to trip an event. Here it is assumed that the upward and downward changes necessary to trip an event are equal; though, that is not strictly necessary. It is not immediately obvious how different the frequency content of the reconstructed voltage will be to that of the events.

5.4 Comparison of Frequency Content

Periodic signals, voltages, events, analytical event rates, and reconstructed voltages were simulated for 5 seconds with timesteps of 1×10^{-4} seconds, $a = 250$, $b = 500$, and $\lambda_r = 0.01$. The signal has a constant component equal to -1 and an amplitude variation for each frequency of 1 stellar magnitude. Figure 3 shows the FFT of the voltage, Figure 4 shows the FFT of the events with $\delta = 0.001$, and Figure 5 shows the FFT of the events with $\delta = 0.1$.

The FFT of the simulated voltage data, Figure 3, clearly reflects the frequency content of the signal. The FFT of the event data, reconstructed voltage, and predicted event rates with a very low event threshold, Figure 4, also clearly show the frequency of the signal; however, they also show components at integer multiples of the frequency due to the "beating" of the event rate. Increasing the event threshold to a more realistic quantity of 0.1, Figure 5 results in a much richer frequency spectrum. The signal frequency can still be detected; however, there are also significant "wings" that appear about 3 Hz above and below the true frequency and much more significant frequency content at higher frequencies. The beating frequencies are less distinct. These results motivate using low event trigger thresholds and imply that one must exercise caution when interpreting the frequency content of event camera data. The reconstructed voltage does not appear to outperform the event data.

6. EMPIRICAL DATA

The VADeR Lab observatory has been routinely acquiring event camera data of satellites in LEO and GEO. The event camera and observatory have been described in detail by Benson & Holzinger [2, 1] and will only be summarized briefly here. The event camera is a Prophesee EVK3 GEN 4.1 which is a 1280 by 720 pixel array. The event camera is mounted on a Officina Stellare RH200 0.2 m f/3 optical tube and is outfitted with an array of filters though none were used in this work.

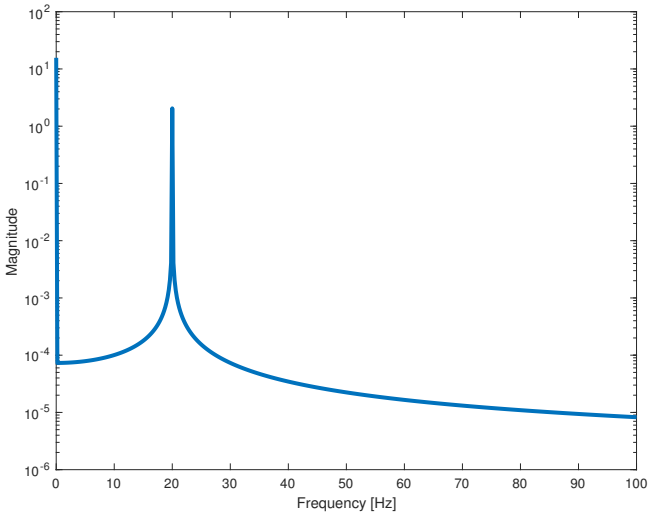

Fig. 3: FFT of simulated voltage data.

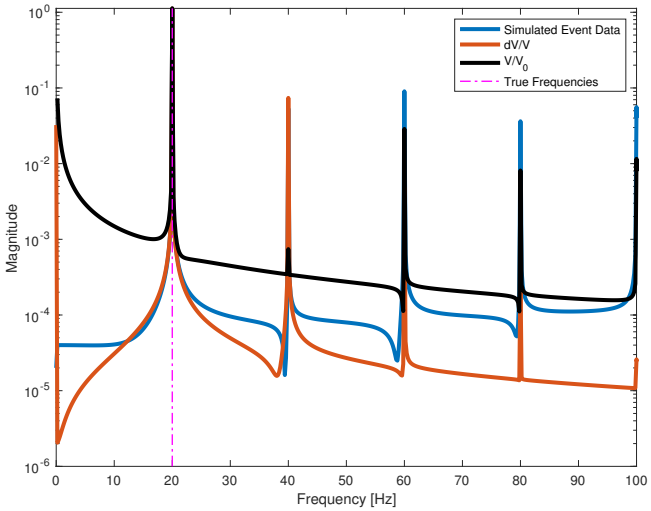

Fig. 4: Normalized FFT of simulated idealized event data, analytical event rates, and reconstructed voltage history on a logarithmic scale. $\delta = 0.001$

Data from the event cameras can be exported of tables containing the pixel coordinates, event timestamp, and event polarity. Images can be constructed by summing the number of events, regardless of polarity, in each pixel for visualization purposes. GEO satellites and other bright satellites of opportunity are regularly observed. Figure 6 shows rate-tracked event data for Cosmos 2227. The faint background streaks are background stars. The events were recorded over a 10.97 second period. Note that precise rate tracking is needed for frequency analysis as if the satellite wanders in the field the frequency content will be superimposed on the signature of the moving point-spread function.

The frequency content of the Cosmos 2227 data was analyzed in a three different ways. First the FFT of events in a very active pixel was taken. In this case that pixel had 180 events over the observation period. The second is simply to sum the events at each timestep, inclusive of polarity, in a 12 by 13 pixel box surrounding the satellite and to take the FFT of that data. The final method investigated was to take the FFT of each pixel individually and add the frequency content in quadrature. The results for this dataset are shown in Fig. 7.

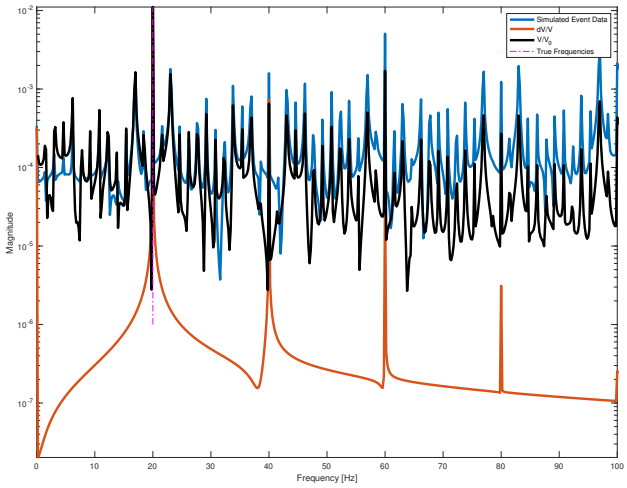

Fig. 5: Normalized FFT of simulated idealized event data, analytical event rates, and reconstructed voltage history on a logarithmic scale. $\delta = 0.1$

The single pixel and added event curves have comparable amounts of noise, while the binned frequency magnitudes curve has much less noise. Interestingly, the single pixel does not seem to have any significant frequency content that is also reflected in the other curves. This suggests that some type of binning is necessary to recover frequency content from the event data. There is a significant signal at 12.4 and 13.4 Hz in both of the binned cases. Interestingly, there are low frequency peaks at 1.8 and 3.5 Hz in the binned magnitude spectrum that are not present in the binned event spectrum. It is unclear if the peaks are real or artifacts of noise. There also appear to be peaks in all three spectra at 5.4 and 17.3 Hz, as well as other minor peaks that are closer to the noise floor. Similarly, the observed frequencies may be from vibrational modes of the spacecraft, atmospheric turbulence, or mount/building vibrations. Further research is needed to rule out these sources. Due to LEO passes occurring sporadically and with significant variation in brightness, it is difficult to reproduce observations; however, the rich spectrum of Cosmos 2227 is encouraging.

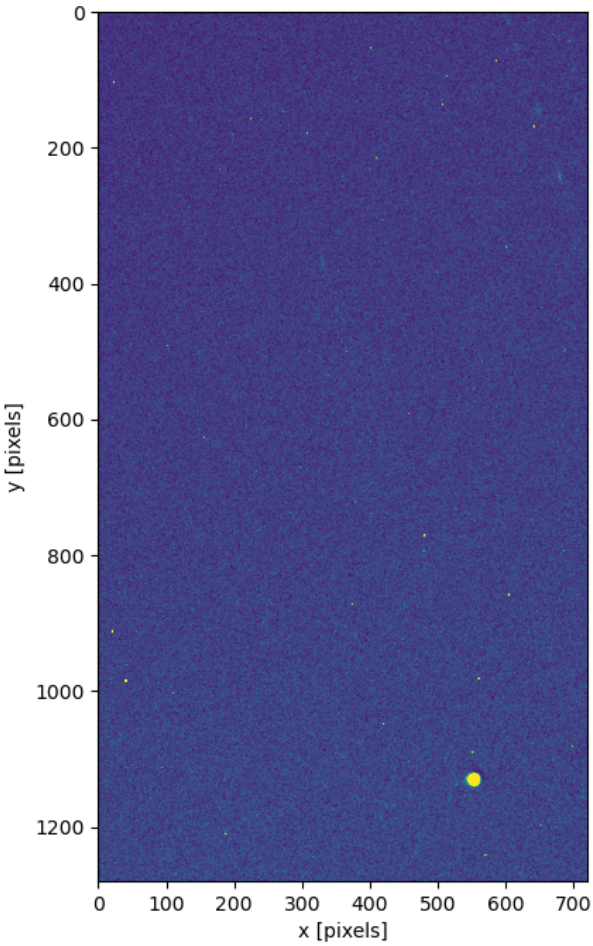

Fig. 6: Cosmos 2227 as seen on June 6th 2024.

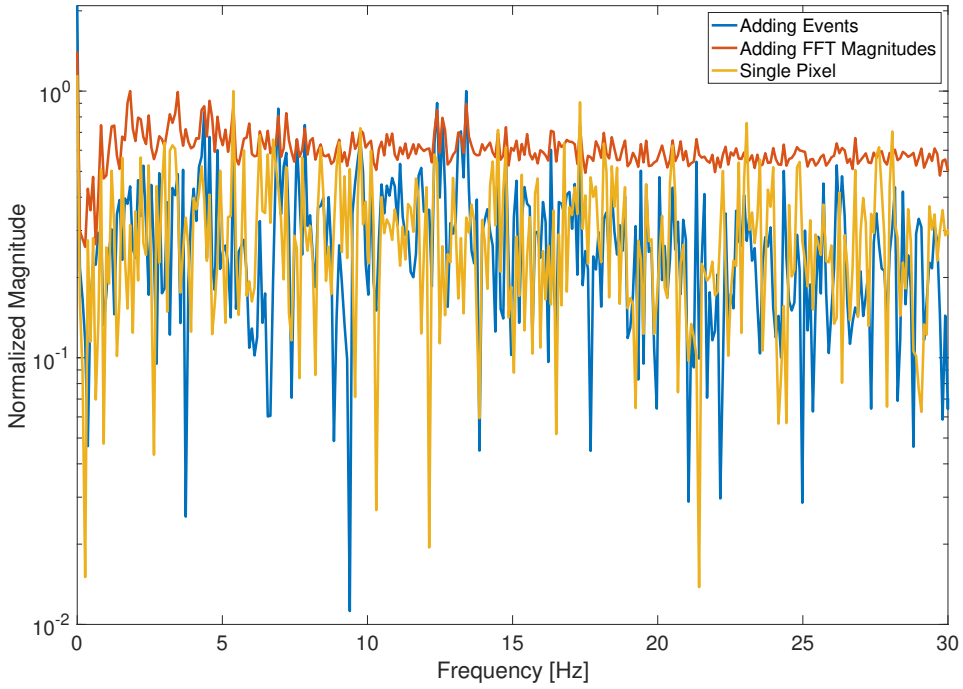

Fig. 7: Frequency content of the Cosmos 2227 observations acquired on June 6th 2024.

7. CONCLUSIONS

This paper derived a transfer function to describe the event camera circuit and used that transfer function to gain insights into the recoverability of periodic signals from event data. These results were used in tandem with analytical results from Benson & Holzinger [2, 1] to inform the tuning parameters, brightness, and brightness variations necessary to detect periodic brightness variations. It was found that the reference flux and decay rate were important for translating brightness variations to voltage variations.

Next, the mean steady state voltage under a periodic input was used to generate idealized events, as well as to calculate analytical event rates. The analytical event rates involves multiple frequencies and this results in beating that produces more frequencies in the output than are present in the signal, which are also reflected in the idealized events. A proxy voltage, as originally done by Benson & Holzinger [2], was constructed from the event data; however, that reconstructed voltage did not result in better frequency content recovery. It was also noted that small event thresholds are better than larger thresholds for frequency content detection, at the cost of more events.

Finally, the frequency spectrum of Cosmos 2227 was investigated using VADeR Lab observatory data. The frequency content of a bright pixel was presented and compared to binned frequency spectra. The binning was done two ways. First, the events in the pixels of interest were summed, inclusive of polarity, at each timestep before the FFT was applied. Second, the FFT of each pixel of interest was calculated and their magnitudes were added in quadrature. The binned spectrum of the magnitudes added in quadrature had significantly less noise than the other spectra. The binned spectra displayed some similarities and some differences to each other and the individual pixel spectrum. The rich frequency content of Cosmos 2227 is encouraging but must be approached with caution. Future work will improve the calibration of event data to isolate frequency content from the satellite from other effects.

ACKNOWLEDGMENTS

The authors are grateful to the VADeR Lab observing team; Chrisanne Kuester, Kyle Bowen, Zackary Goldberg, and Owen Schuler, for acquiring the event camera data used in this work. This work was funded through the AFOSR Space University Research Initiative program.

REFERENCES

[1] Conor Benson and Marcus Holzinger. Simulation and analysis of event camera data for non-resolved objects. *The Journal of the Astronautical Sciences*, 71(1):3, 2023.

[2] Conor J Benson and Marcus J Holzinger. Simulation and analysis of event camera data for non-resolved objects. In *Proceedings of the Advanced Maui Optical and Space Surveillance Technologies Conference, Maui, HI*, 2022.

[3] Conor J Benson, Daniel J Scheeres, William H Ryan, and Eileen V Ryan. Cyclic complex spin state evolution of defunct geo satellites. In *Proceedings of the Advanced Maui Optical and Space Surveillance Technologies Conference, Maui, HI*, 2018.

[4] Patrick Lichtsteiner, Christoph Posch, and Tobi Delbruck. A 128×128 120 db 15μs latency asynchronous temporal contrast vision sensor. *IEEE journal of solid-state circuits*, 43(2):566–576, 2008.